ARTICLE
Journal of Cellular Biochemistry 109:184–195 (2010)

Journal of Cellular Biochemistry

Suberoylanilide Hydroxamic Acid (SAHA) at Subtoxic Concentrations Increases the Adhesivity of Human Leukemic Cells to Fibronectin

Kateřina Kuželová,* Michaela Pluskalová, Barbora Brodská, Petra Otevřelová, Klára Elknerová, Dana Grebeňová, and Zbyněk Hrkal

Department of Cellular Biochemistry, Institute of Hematology and Blood Transfusion, Prague, Czech Republic

ABSTRACT

Suberoylanilide hydroxamic acid (SAHA) is an inhibitor of histone deacetylases (HDACs) which is being introduced into clinic for the treatment of hematological diseases. We studied the effect of this compound on six human hematopoietic cell lines (JURL-MK1, K562, CML-T1, Karpas-299, HL-60, and ML-2) as well as on normal human lymphocytes and on leukemic primary cells. SAHA induced dose-dependent and cell type-dependent cell death which displayed apoptotic features (caspase-3 activation and apoptotic DNA fragmentation) in most cell types including the normal lymphocytes. At subtoxic concentrations (0.5–1 μM), SAHA increased the cell adhesivity to fibronectin (FN) in all leukemia/lymphoma-derived cell lines but not in normal lymphocytes. This increase was accompanied by an enhanced expression of integrin β1 and paxillin, an essential constituent of focal adhesion complexes, both at the protein and mRNA level. On the other hand, the inhibition of ROCK protein, an important regulator of cytoskeleton structure, had no consistent effect on SAHA-induced increase in the cell adhesivity. The promotion of cell adhesivity to FN seems to be specific for SAHA as we observed no such effects with other HDAC inhibitors (trichostatin A and sodium butyrate). J. Cell. Biochem. 109: 184–195, 2010.

KEY WORDS: SUBEROYLANILIDE HYDROXAMIC ACID; ADHESION; HEMATOPOIETIC CELL; APOPTOSIS; INTEGRIN; PAXILLIN

The acetylation status of core histones resulting from the antagonistic activities of histone deacetylases (HDACs) and histone acetyltransferases (HATs) represents an important regulatory element of gene transcription [Monneret, 2005]. HDACs are recruited to target genes via their association with transcription activators and repressors, as well as their incorporation into large multiprotein complexes. Although diminished histone acetylation at promoter regions generally correlates with gene silencing, there is also evidence that HDACs can activate some genes [Haberland et al., 2009]. Deletion or inhibition of HDACs often results in the upregulation or downregulation of approximately equivalent percentages of genes. In addition to histones, at least 50 other proteins with known biological function are substrates for HDACs. The mammalian nonhiston HDAC substrates comprise transcription factors with DNA-binding affinity (e.g., p53, c-Myc, E2F, BCL-6, GATA), other transcription regulators (e.g., Rb protein), signal transmitters, DNA reparating enzymes, chaperones (e.g., HSP90), or cytoskeletal proteins (α-tubulin).

Suberoylanilide hydroxamic acid (SAHA, other names: Vorinostat, Zolinza) is the first member of the group of HDAC inhibitors which has received Food and Drug Administration approval for treating patients with cutaneous T-cell lymphoma in the USA [Duvic and Vu, 2007; Marks and Breslow, 2007]. While it is also evaluated in clinical trials for the treatment of other oncological and hematological diseases [O'Connor et al., 2006; Crump et al., 2008; Modesitt et al., 2008; Richardson et al., 2008], the mechanism of its action is largely unexplained [Xu et al., 2007]. This is equally true for other HDAC inhibitors which can be divided into several structural classes including short-chain fatty acids (e.g., sodium butyrate, valproic acid,. . .), hydroxamates (SAHA, trichostatin A,. . .), cyclic peptides (trapoxin A, depsipeptid,. . .), and benzamides (MS275,. . .) [Dokmanovic et al., 2007].

In a general way, HDAC inhibitors can induce proliferation arrest, terminal differentiation, or death of transformed cells. The latter process can resemble apoptosis, mitotic catastrophe, autophagy, senescence, or reactive oxygen species-mediated cell death [Ruefli

Grant sponsor: Grant Agency of the Czech Republic; Grant number: 301/09/1026; Grant sponsor: Grant Agency of the Ministry of Health, Czech Republic; Grant number: NR/9243-3.

*Correspondence to: Dr. Kateřina Kuželová, Department of Cellular Biochemistry, Institute of Hematology and Blood Transfusion, U Nemocnice 1, 128 20 Prague 2, Czech Republic. E-mail: kuzel@uhkt.cz

Received 4 September 2009; Accepted 30 September 2009 • DOI 10.1002/jcb.22397 • © 2009 Wiley-Liss, Inc.
Published online 12 November 2009 in Wiley InterScience (www.interscience.wiley.com).

et al., 2002; Mitsiades et al., 2004; Rosato and Grant, 2004; Shao et al., 2004; Yu et al., 2005; Lindemann et al., 2007]. The cell response to the treatment with a HDAC inhibitor is variable depending on the individual inhibitor, the dose, the treatment time, and on the cell type. In any case, the effects are pleiotropic and include activation or inactivation of multiple signaling pathways. SAHA binds to Zn^{2+} in the active site of individual HDACs belonging to classes I and II and often induces mitochondrial apoptosis governed by Bcl-2 protein family. It has been suggested that the apoptosis can be triggered as a result of DNA damage caused by HDAC inhibitors [Gaymes et al., 2006]. Activation of the extrinsic apoptotic pathway has also been reported [Gillenwater et al., 2007]. The changes in the gene expression upon treatment of cell lines or patient primary cells with SAHA have been studied prevalently using DNA microarrays [Glaser et al., 2003; Peart et al., 2005; Desmond et al., 2007; Tavares et al., 2008; Kumagai et al., 2009]. In the individual reports, the transcription rate was found to be altered in 2–10% of all expressed genes. However, the attempts to identify the altered genes on both RNA and protein levels [Tong et al., 2008] have given only moderate overlap among different cell systems. The most consistent change occuring after SAHA treatment seems to be the induction of the cell cycle regulators p21 and p27 resulting in cell cycle arrest which protects the cell against the toxic effects of the drug [Gui et al., 2004]. At higher SAHA concentration or as a result of simultaneous inhibition of MEK/ERK and Akt transduction pathways, mitochondrial apoptosis is usually triggered. The mechanism of cell death often, but not systematically, involves the production of reactive oxygen species [Marks and Jiang, 2005; Xu et al., 2007; Brodská et al., 2009].

In this work, we report on changes in cellular adhesivity to fibronectin (FN), an essential component of bone marrow extracellular matrix (ECM), which were induced by SAHA in human hematopoietic cells. We describe the effects of SAHA on the expression of integrin β1 on the cell surface as well as on the expression level of paxillin, a characteristic member of focal adhesions, that is, the protein complexes which are assembled around the cytoplasmic parts of integrins upon cell binding to the ECM. We also studied the role of the proteins ROCK in these processes and concluded that this regulators of actin cytoskeletal structure are not essentially involved in the observed SAHA-induced increase of cellular adhesivity to FN.

MATERIALS AND METHODS

CHEMICALS

SAHA was supplied by Alexis (San Diego, USA). Human FN (alpha-chymotryptic fragment, 120 K) was purchased from Chemicon International (CA, USA), anti-paxillin antibody (clone 5H11) from Millipore (Upstate). The labeled antibodies against integrins β1 (CD29) and β2 (CD18) were from Chemicon International and Exbio (Prague, Czech Republic), respectively. Anti-actin antibody, FITC-labeled phalloidin, and the fluorogenic substrate Ac-DEVD-AFC were obtained from Sigma (Prague, Czech Republic). The inhibitor Y-27632 which inhibits ROCK1 and ROCK2 was from Calbiochem.

CELL CULTURE AND LYMPHOCYTE PREPARATION

JURL-MK1, CML-T1, and Karpas-299 cells were purchased from DSMZ (German Collection of Microorganisms and Cell Cultures, Braunschweig, Germany), K562 and HL-60 cell lines from the European Collection of Animal Cell Cultures (Salisbury, UK). The cells were cultured in RPMI 1640 medium supplemented with 10% fetal calf serum, 100 U/ml penicillin, and 100 μg/ml streptomycin at 37°C in 5% CO_2 humidified atmosphere.

Blood samples were prepared from buffy coats taken from healthy volunteers or from the whole blood of patients with chronic myelogenous leukemia (CML) or acute myeloid leukemia (AML) following their written informed consent. Peripheral blood mononuclear cells were isolated by standard density gradient centrifugation using Histopaque®-1077 (Sigma). Monocytes were depleted by overnight culture in plastic flasks and by harvesting of nonadherent cells. The lymphocytes were further maintained in RPMI 1640 medium as described above for the cell lines. The fraction of CD34-positive cells in the bone marrow of CML patients was from 1% to 3%.

ADHESION ASSAY

The extent of cell adhesivity to FN was assessed by fluorometric quantitation of cells attached to FN-coated wells of a microtitration plate. The fraction of adherent cells was determined by comparing the fluorescence signal arriving from FN-coated plate with that from a reference plate containing the total cell amount. To prepare the coated plate, 50 μl of FN solution (20 μg/ml in distilled water) was added to each well of a Nunc Maxisorp microtitration plate which was subsequently incubated overnight in the cold. Then, the wells were washed three times in PBS and the remaining protein adherence sites were blocked by 200 μl 1% BSA in PBS for at least 30 min at room temperature. The plate was washed once again in PBS and 100 μl of cell suspension at a density of 1×10^5 cells/ml was added to the wells in quadruplicates. The cell density used in the assay was determined as a good compromise between the need to obtain sufficiently high fluorescent signal and the effort to minimize the effects of cell–cell interactions on the results of the assay. The same amount of cells was added in quadruplicates to the reference plate. A special care was taken of frequent gentle mixing to assure high homogenity of the suspension. The FN-coated plate was shortly centrifuged (350*g* for 2 min) and incubated for 1 h at 37°C. Then, the culture medium was uniformly aspirated using a multichannel adaptor to the suction-pump (Sigma), the wells were filled with 200 μl PBS/Ca^{2+}/Mg^{2+} (PBS, pH 7.4, supplemented with 1 mM Ca^{2+} and 1 mM Mg^{2+}) using a multichannel pipette, the plate was re-aspirated and frozen at −70°C. In the meantime, the reference plate was centrifuged at 400*g* for 10 min to pellet the cells, gently inverted (bottom-up), the medium was tapped-out, the plate was shortly blotted onto a paper towel and frozen at −70°C.

Cy-Quant Cell Proliferation Assay Kit (Molecular Probes) was used to quantitate the samples according to manufacturer's instructions. Briefly, the plates were thawed (10 min at room temperature), 200 μl of dye/cell lysis solution was added to each well including four blanks (without cells) and the plates were incubated for 10 min in the dark. The well fluorescence (excitation at 485 nm, emission at 520 nm) was measured, the quadruplicates were

averaged and the adherent cell fraction (ACF) was calculated as follows:

$$ACF = \frac{F_{FN} - F_B}{F_{REF} - F_B} \times 100\%$$

where F_{FN}, F_{REF}, and F_B are the average fluorescence intensities of the wells from FN-coated plate, reference plate, and blanks, respectively.

The standard error of quadruplicates was typically of 3–8% of the measured value.

CASPASE-3 ACTIVITY ASSESSMENT

The activity of caspase-3 was determined by fluorometric measurement of the kinetics of 7-amino-4-trifluoromethyl coumarin (AFC) release from the fluorogenic substrate Ac-DEVD-AFC in the presence of cell lysates. The method was described in detail in Kuželová et al. [2007]. After the incubation with 0.5 or 2 μM SAHA the cells were washed and lysed and aliquots of cytosolic fractions were incubated for 30 min at 37°C with the fluorogenic substrate. The linear increase of fluorescence intensity at 520 nm was monitored during this incubation time using Fluostar Galaxy microplate reader (BMG Labtechnologies, Germany).

FLOW CYTOMETRY ANALYSIS

Flow cytometry measurements were performed on Coulter Epics XL flow cytometer.

The fraction of cells containing apoptotic DNA breaks was measured by TUNEL assay using the In Situ Cell Death Detection Kit, Fluorescein (Roche Diagnostics GmbH, Mannheim, Germany) following the standard manufacturer's protocol.

To analyze the expression level of integrins on the cell surface, the cells (5×10^5) were washed in PBS and stained with 5 μl PE-conjugated anti-integrin β1 or 10 μl FITC-conjugated anti-integrin β2 antibody. After 40 min incubation at room temperature, the cells were washed twice in PBS and the fluorescence histograms of red or green fluorescence were recorded using the flow cytometer.

To stain the actin polymers, the cells were washed in PBS and fixed and permeabilized using FIX&PERM cell permeabilization kit from An Der Grub (Kaumberg, Austria). Washing steps were performed in PBS supplemented with 1% BSA using short centrifugation times (2 min at 350*g*). FITC-labeled phalloidin (3 μl) was added to cells suspended in 50 μl PERM solution. The samples were incubated for 40 min at room temperature, washed in PBS + 1% BSA and the green fluorescence was measured using the flow cytometer.

RNA EXTRACTION AND RT-PCR

The extraction of RNA from cells cultured in the absence or presence of 0.5 μl SAHA was carried out using the RNeasy Mini Kit (Qiagen, Inc., Valencia, CA) in accordance with the manufacturer's instructions. The purified RNA was stored at −75°C until use. Semi-quantitative RT-PCR was performed using 2 μg of total RNA and One-Step RT-PCR kit (Qiagen). The sequences of specific primers (Invitrogen) were designed using the Primer-BLAST software available in NCBI database as follows: integrin β1—GCGCGGAAAAGATGAATTT (forward) and CCCCTGATCTTAATCGCAAA (reverse); paxillin transcription variant 2—CCATCACTGTGAACCAGGG (forward) and TTTCACAGTAGGGCTGTCCA (reverse). The RT-PCR program applied on Techne Cyclogene thermocycler (Techne, Cambridge, UK) was: 30 min at 50°C for reverse transcription, 15 min at 95°C for HotStarTaq DNA polymerase activation, Omniscript and Sensiscript reverse transcriptases inactivation and the cDNA template denaturation followed by 20–30 cycles consisting of 1 min denaturation at 94°C, 1 min of annealing at 60°C, and 2 min of extension at 72°C. The program was terminated by a final extension of 10 min at 72°C. Amplified products were detected on electrophoretic agarose gels containing 0.5 μg/ml of ethidium bromide. The integrated intensities of fluorescent bands were obtained using the Molecular Imager Gel Doc XR System (Bio-Rad Laboratories, Inc., Hercules, CA) and analyzed using AIDA 1D v. 4.08 evaluating software (Raytest GmbH, Straubenhardt, Germany). In all experiments, α-actin was used as the loading standard and the integrated fluorescent intensities of studied bands were corrected to small differences in the amount of total RNA loaded using the values from actin bands.

ELECTROPHORESIS AND WESTERN BLOTTING

The SDS electrophoresis and Western blotting were performed using the protocols which were described previously [Kuželová et al., 2007]. The protein concentration was measured using a Bio-Rad protein assay (Bio-Rad Laboratories). As a rule, 15 μg total protein was applied to each well. Actin band was used as a control of equal protein loading.

RESULTS

We studied the effects of SAHA on different leukemic cell lines as well as on lymphocytes from healthy donors. The cell lines included three lines derived from patients with CML (JURL-MK1, K562, and CML-T1) and lines derived from human AML (HL-60) and human T-cell lymphoma (Karpas-299). Treatment with SAHA induced a decrease of the cell proliferation rate, which was similar for all the studied cell lines (data not shown) and cell death. The cytotoxic effects were strongly dose-dependent and cell type-dependent. Figure 1 shows the extent of DNA fragmentation, a characteristic marker of apoptosis, after 48 h treatment of cells with SAHA at different concentrations. DNA from control and treated cells was analyzed using TUNEL method which consists in fluorescent labeling of apoptotic DNA breaks. We also assessed the activation of caspase-3, another hallmark of apoptosis, using the fluorogenic caspase-3 substrate, Ac-DEVD-AFC. Figure 2A shows the kinetics of caspase-3 activation in JURL-MK1 cells treated with 0.5 or 2 μM SAHA. Similar kinetics was seen in the other cell lines. The values of caspase-3 activity in different cell lines after 28–30 h treatment (i.e., time of maximal activity) with 0.5 or 2 μM SAHA are given in Figure 2B.

Although SAHA triggers apoptosis in many cell types including normal lymphocytes, other forms of cell death are also likely to be induced by the treatment. Figure 3 shows the fraction of dead cells (i.e., cells not able to exclude the Trypan-blue dye) resulting from 48 h treatment of different cell lines with 0.5 or 2 μM SAHA. The cell

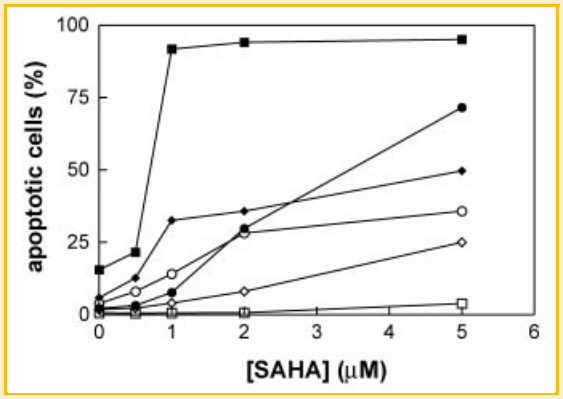

Fig. 1. Apoptotic DNA fragmentation induced by SAHA in different leukemic cell lines and donor lymphocytes. Cells were treated with SAHA at different concentrations for 48 h, harvested and stained with fluorescein-dUTP using TUNEL method to obtain the fraction of cells with apoptotic DNA breaks. Different symbols correspond to different cell lines: K562 (open squares), HL-60 (closed squares), JURL-MK1 (closed circles), Karpas-299 (open diamonds), CML-T1 (closed diamonds), and donor lymphocytes (open circles).

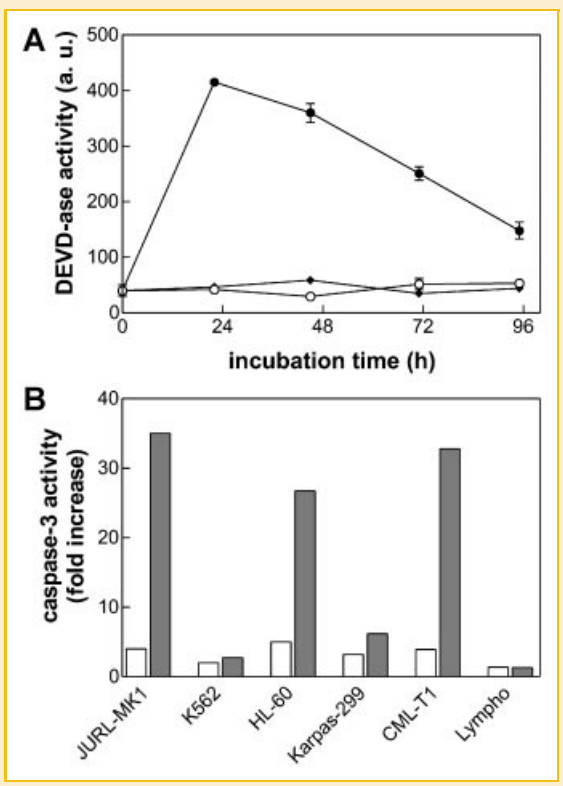

Fig. 2. Caspase-3 activation in SAHA-treated leukemic cells and donor lymphocytes. The cells were treated with 0.5 or 2 μM SAHA for different time intervals and the activity of caspase-3 in cell lysates was assessed using the fluorogenic caspase-3 substrate Ac-DEVD-AFC. Panel A: The kinetics of caspase-3 activation in JURL-MK1 cells treated with SAHA at 0.5 μM (diamonds) or 2 μM concentration (closed circles). Open circles: JURL-MK1 cells without treatment. Panel B: The maximal values of caspase-3 activity after treatment with SAHA 0.5 μM (clear bars) or 2 μM (dark bars) for different cell lines and donor lymphocytes. The results are expressed as ratios of caspase-3 activity in treated cells and in the controls.

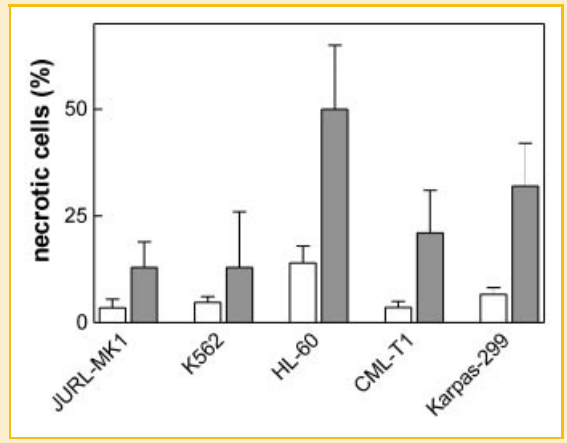

Fig. 3. Cell death induced by SAHA in different cell lines. The cells were treated with 0.5 μM (clear bars) or 2 μM (dark bars) SAHA for 48 h and the fraction of Trypan blue-positive cells was determined by cell counting. The results are means and standard deviations from 4 to 15 independent experiments.

lines Karpas-299 and K562, which are relatively resistant to SAHA-induced apoptosis, are also damaged by 2 μM SAHA treatment. On the other hand, no significant toxicity was observed when SAHA was used at 0.5 μM concentration. Although HL-60 cells are more sensitive to SAHA-induced cell death in comparison with the other cell types, the difference between controls and samples treated with 0.5 μM SAHA is not large (HL-60 cells display relatively high level of spontaneous apoptosis even without treatment and the fraction of Trypan blue-positive cells in controls is also higher compared to controls from other cell types).

We noted during our studies on adhesion properties of leukemic cells that SAHA alters the cell adhesivity to FN. Normal hematopoietic cells are retained in the bone marrow until their maturation and release into the blood circulation. The main contribution to the attachment forces is provided by the interaction of cellular β integrins, transmembrane glycoproteins, with protein components of ECM. We performed the analysis of integrin composition in JURL-MK1 and K562 cells using Beta Integrin-Mediated Cell Adhesion Array kit (Fig. 4A) and compared the interaction of these cells with different ECM proteins using Cytomatrix Screen kit (Fig. 4B). We concluded from these results that the most relevant interaction partners for cell attachment to ECM are integrins β1 and β2 and FN. We thus used microtitration plates coated with FN for subsequent study of the effects of SAHA on cell adhesion to ECM. The protocol we adopted allows for sensitive and reproducible determination of the cell fraction which remained attached to FN after the plate washing (ACF). As the ACF varies between different cell types, the results were also expressed as a ratio of ACF values obtained from treated samples and the corresponding controls. This representation is used in Figure 5 which shows the effect of SAHA at different concentrations (48 h treatment) on the adhesion of cell lines and normal lymphocytes to FN. SAHA increased the ACF in all studied cell lines but not in normal lymphocytes. This effect was usually maximal at 0.5–1 μM SAHA concentration while higher SAHA doses were less effective. The only

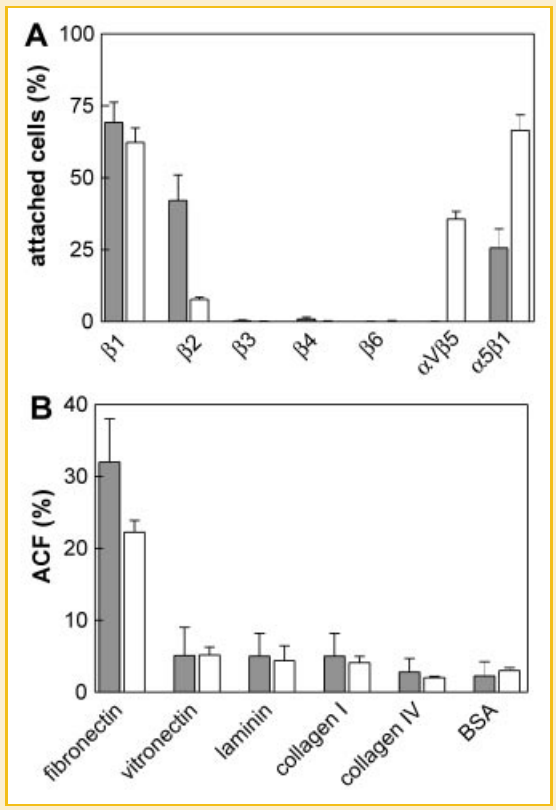

Fig. 4. Analysis of β-integrin expression on the surface of JURL-MK1 and K562 cells and of the cell interaction with different ECM proteins. Panel A: JURL-MK1 (dark bars) and K562 (clear bars) cell attachment to wells coated with antibodies against different β-integrins was studied using Beta Integrin-Mediated Cell Adhesion Array kit. Panel B: The fraction of JURL-MK1 (dark bars) and K562 (clear bars) cells which adhere to wells coated with different ECM proteins was obtained using Cytomatrix Screen kit.

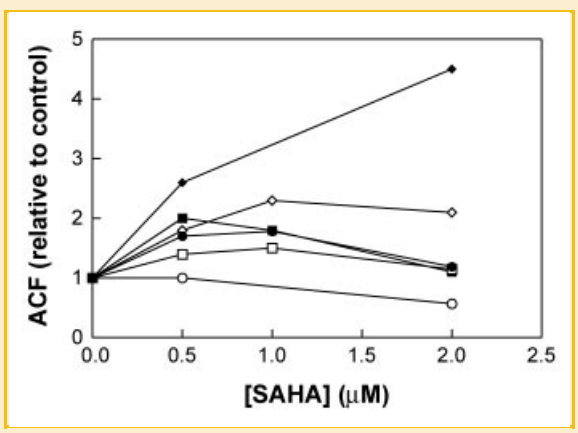

Fig. 5. Effect of SAHA on the extent of cell adhesion to fibronectin. The cells were treated for 48 h with SAHA at different concentrations and the adherent cell fraction (ACF) was determined using fluorometric determination of the quantity of cells which remained attached to fibronectin-coated wells of a microplate after the plate washing. The represented results are expressed as ratios of ACFs from treated cells and ACFs from the appropriate controls. The legend to symbols is the same as in Figure 1: K562 (open squares), HL-60 (closed squares), JURL-MK1 (closed circles), Karpas-299 (open diamonds), CML-T1 (closed diamonds), and donor lymphocytes (open circles).

exception is represented by CML-T1 cells which also distinguishes from other cell lines by markedly lower adhesivity (ACFs in controls are 2–4% compared to about 30–40% for other cell lines). In subsequent experiments, we focused on 0.5 μM SAHA which increased the adhesivity in all cell lines without exhibiting significant toxicity and we collected a large set of data for six cell lines (including the previously specified ones and AML cell line ML-2) and primary lymphocytes (Table I). The treatment time was fixed to 48 h as the maximal effect was achieved at this time, although increase in ACF occurred already after 24 h treatment. It follows from the statistical analysis of these data that SAHA-induced increase in the cell adhesivity is significant and similar for all leukemia cell lines regardless of their origin while no effect is produced in normal lymphocytes under the same experimental conditions. A slight but statistically significant increase in cell adhesivity was also found in primary cells from CML patients. We tested in addition three primary samples from acute myelogenous leukemia (AML) patients, but the results were inconclusive (26% increase due to SAHA in one of them and 36%, resp. 50% decrease in two others).

As the cell interaction with FN appears to be mainly mediated by integrin β1, we wondered if SAHA alters the expression of this protein on the cell surface. JURL-MK1, K562, Karpas-299, CML-T1, and HL-60 cells were thus treated with 0.5 μM SAHA for 48 h, stained with fluorescently labeled anti-integrin β1 antibody and analyzed using a flow-cytometer. Firstly, we inspected the scattergrams, that is, plots of side-scattered light intensity (SSC), versus forward-scattered light intensity (FSC) which were usually not significantly altered by the treatment with SAHA. This indicates that SAHA at 0.5 μM concentration does not induce changes in the cell size and shape which is in agreement with the lack of toxicity under these conditions (data not shown). In some experiments, especially in those with HL-60 cells, a distinct cell subpopulation was present at lower FSC and higher SSC. This probably reflects apoptotic cell shrinkage and membrane blebbing occurring in a small cell fraction. Subsequently, we analyzed the expression of β1 integrin on the cell surface using PE-conjugated anti-β1 integrin antibody. Representative histograms of fluorescence intensities obtained following the cell staining are given in Figure 6. A shift towards higher fluorescence intensities was repeatedly observed after treatment of JURL-MK1, K562, Karpas, and CML-T1 cells with SAHA. The average increase in the mean fluorescence intensity (MFI) from repeated experiments is also indicated in the figure. In the case of HL-60 cells, no consistent change of MFI was observed for the "intact" cells (i.e., those with unchanged scattering properties) while the altered cell subpopulation (lower FSC, higher SSC) displayed slightly decreased staining of β1 integrin (data not shown). We also explored the expression of β2 integrin using a FITC-conjugated antibody, but the fluorescence signal obtained in this case was very weak indicating that the expression of β2 integrin is low in comparison with that of β1 in our model systems.

In adherent cells, the engagement of integrins leads to the formation of large multiprotein complexes, so-called focal adhesions, at the cytoplasmic side of the cell membrane. Antibodies against one characteristic component of these complexes, the protein paxillin, are often used for staining of focal adhesions. We used an anti-paxillin antibody to reveal possible changes in paxillin

TABLE I. Effect of SAHA on the Cell Adhesion to Fibronectin

	ACF in controls (%)	Average increase after SAHA (fold of control)	Number of experiments	P-value	Significant difference ($P < 0.05$)
JURL-MK1	38 ± 19	1.7 ± 0.4	17	<0.0001	Yes
K562	38 ± 22	1.5 ± 0.3	11	0.0003	Yes
HL-60	26 ± 21	2.5 ± 1.5	11	0.0003	Yes
Karpas-299	32 ± 22	1.8 ± 0.7	9	<0.0001	Yes
ML-2	32 ± 23	2.0 ± 1.0	6	0.0077	Yes
CML-T1	3.6 ± 3	2.3 ± 0.6	11	0.0012	Yes
Normal lymphocytes	35 ± 8	1.0 ± 0.2	10	0.3188	No
CML lymphocytes	34 ± 16	1.16 ± 0.13	6	0.0214	Yes

The cells were treated with 0.5 μM SAHA for 48 h and subjected to adhesion assay. The values of adherent cell fraction (ACF) and of the average increase in ACF due to SAHA are given as means and standard deviations of repeated experiments. The experiments using primary cells were completely independent (samples obtained from different individuals). Clinical samples were obtained from previously untreated patients with chronic myelogenous leukemia (CML). P values for the difference between controls and SAHA-treated samples were computed using the standard two-tailed paired t-test.

content resulting from the treatment of cells with SAHA. Western blots from cell lysates show an increase in paxillin expression following SAHA treatment for all cell lines that we tested (Fig. 7). Moreover, an additional band at slightly higher MW which is also recognized by anti-paxillin antibody appears as a result of SAHA treatment in some cell lines. No change in paxillin expression was observed in normal lymphocytes treated with SAHA.

In order to get insight into the mechanism of β1 integrin and paxillin protein level increase by SAHA, we searched for potential changes at the transcriptional level using specific primers and RT-PCR method in JURL-MK1, Karpas, and CML-T1 cell lines. We found that integrin β1 mRNA levels corresponded well to that of protein product and the increase in β1 expression is thus due to an upregulation of the corresponding mRNA transcription (Fig. 8A,B). The used primers for paxillin should primarily detect the transcription variant 2 (product of 417 bp) which is translated into the ubiquitously expressed paxillin isoform α. In addition, these primers are also able to detect the transcription variant 1 (product of

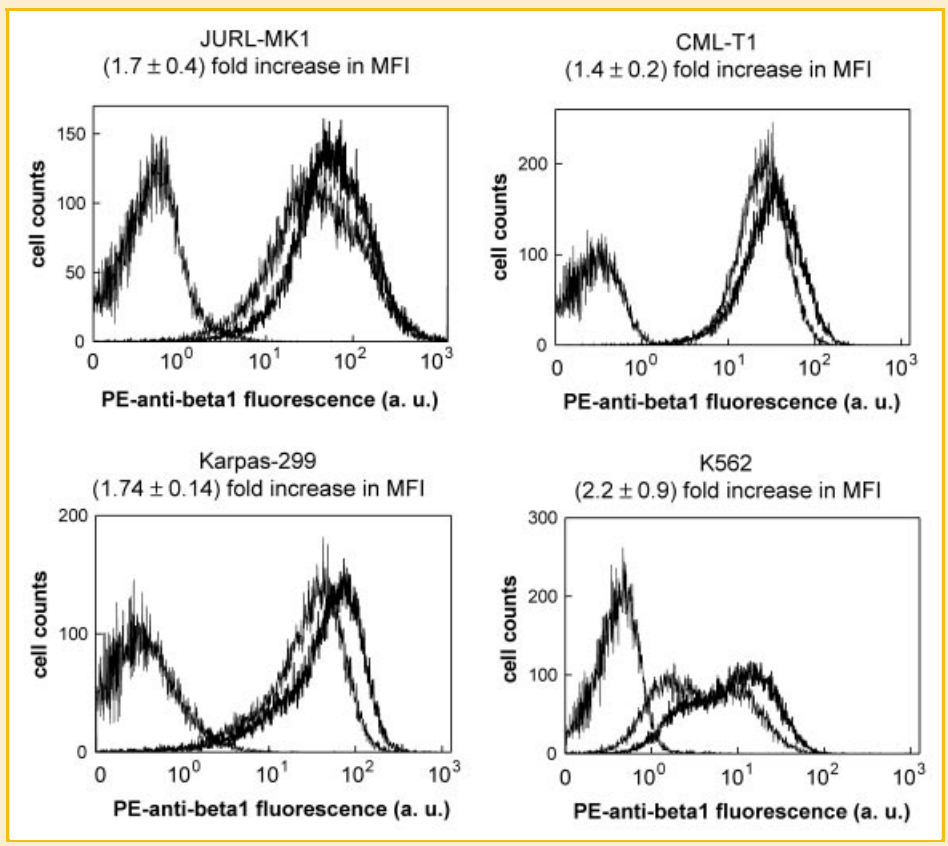

Fig. 6. Effect of SAHA on integrin β1 expression on the cell surface. The cells were treated with 0.5 μM SAHA for 48 h, stained with PE-conjugated anti-β1 integrin antibody and analyzed using a flow-cytometer. The fluorescence intensity from SAHA-treated cells (thicker lines) was higher in comparison with that from control cells. The records on the left side of each panel were from negative controls (no antibody staining). The numbers below the cell line names give the average increase in mean fluorescence intensity (MFI) from four to six independent experiments.

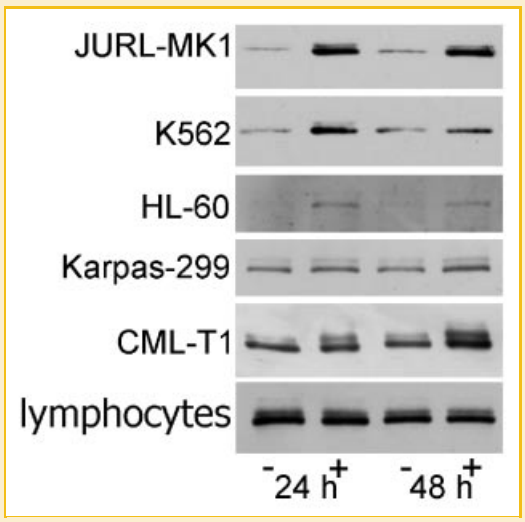

Fig. 7. Changes in paxillin expression induced by SAHA. Cells were incubated for 24 or 48 h as indicated with (+) or without (−) 0.5 μM SAHA. No effect of SAHA treatment was detected on anti-actin blots which were performed as loading controls.

519 bp) coding for paxillin isoform β or γ. Indeed, we observed one dominant band whose intensity increased about 1.5-fold after SAHA treatment and, at higher amplification, an additional band displaying two- to threefold increase due to 24 h 0.5 μM SAHA treatment (Fig. 8A). It thus seems that the increase in paxillin expression level is at least partly due to an upregulation of both paxillin α and paxillin β/γ mRNA.

Focal adhesions not only assure mechanical attachment of the cell to ECM network but represent also communication points which transmit signals from the inside of the cell to ECM and vice versa. The binding of the extracellular parts of integrins to their ligands leads among others to the activation of small GTPases from Rho family, which are considered to be important regulators of the cytoskeleton dynamics, cell adhesion, and migration. In adherent cells, cell adhesion to FN is regulated through the activity of RhoA and its downstream effectors, proteins ROCK1 and ROCK2. In order to reveal possible involvement of ROCK activity in the increase of cell adhesion induced by SAHA, we used the inhibitor Y-27632 which should specifically block the activity of ROCK1 and ROCK2 at 5–10 μM concentration. To confirm the inhibitor efficiency, we tested its effects on the actin polymerization state in the cells using fluorescently labeled phalloidin which binds to actin polymers but not to actin monomers. The treatment of JURL-MK1, K562 or Karpas-299 cells with 10 μM Y-27632 induced a moderate, but reproducible decrease of FITC-phalloidin fluorescence intensity which was not further enhanced by increasing the inhibitor dose (data not shown). This observation is in agreement with the known action of ROCK proteins on the stabilization of actin fibers and indicates that 10 μM Y-27632 is sufficient to inhibit ROCK activity. No effect on the cell viability in any of the studied cell lines was observed using this concentration of the inhibitor.

The effect of Y-27632 on the cell adhesion to FN was strongly cell type-dependent. In CML-T1 and HL-60 cells, 18 h treatment with Y-27632 significantly reduced ACF (Fig. 9). On the other hand, no effect of Y-27632 on JURL-MK1 or Karpas-299 cell adhesion was observed for up to 24 h treatment. Prolonged incubation (48 h) of

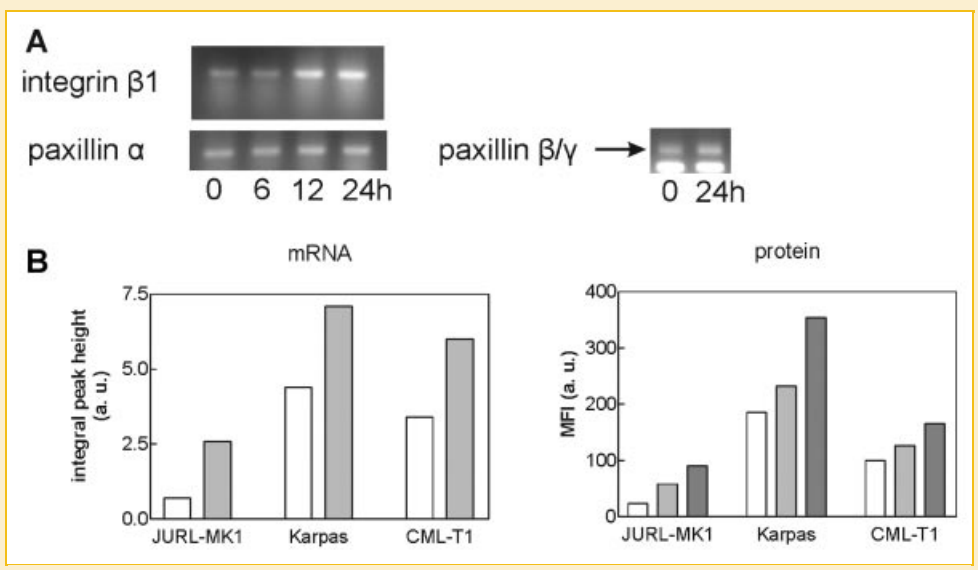

Fig. 8. Changes in mRNA expression levels for integrin β1 and paxillin induced by SAHA. Panel A: JURL-MK1 cells were treated with 0.5 μM SAHA for up to 24 h as indicated and expression levels of integrin β1 and paxillin mRNA were analyzed using RT-PCR method and specific primers. The use of paxillin-specific primers allowed for the detection of one dominant band and an additional band at higher MW, which probably correspond to transcription variants 2 and 1, the templates for paxillin alpha and beta/gamma, respectively. Actin bands were used as loading controls. Panel B: Comparison of SAHA-induced changes in mRNA and protein levels for integrin β1 in JURL-MK1, Karpas-299, and CML-T1 cells. Cells were treated with 0.5 μM SAHA for up to 48 h (clear bars: controls, gray bars: 24 h, dark bars: 48 h). Integrin mRNA expression level was determined using RT-PCR method and normalized using actin mRNA bands. Protein integrin expression on the cell surface was analyzed in parallel from the same samples using fluorescent antibody and flow-cytometry.

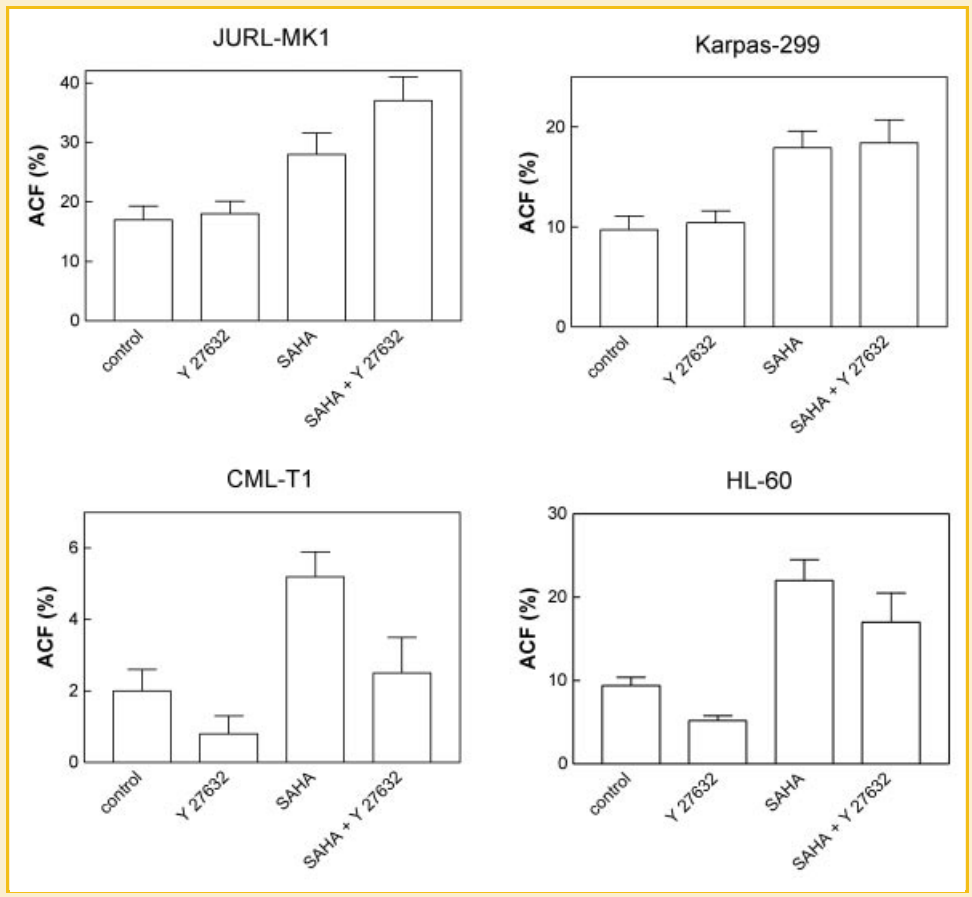

Fig. 9. Representative experiments showing the effects of Y-27632 on cell adhesion to fibronectin. Cells were treated with 0.5 μM SAHA alone or in combination with 10 μM Y-27632 and the adherent cell fraction (ACF) was measured using the adhesion assay. Legend to bar labels: control: untreated cells, Y-27632: treated for 24 h with Y-27632, SAHA: treated for 48 h with SAHA, SAHA + Y-27632: treated with SAHA for 48 h, Y-27632 was added for the last 24 h. The results from repeated experiments are summarized in Table II.

control JURL-MK1 cells with Y-27632 produced inconsistent effects on the cell adhesion (no change, increase or decrease were observed in multiple experiments) and we thus limited the use of the inhibitor to 24 h treatment as the maximum. To test the influence of Y-27632 on SAHA-induced increase of ACF, the cells were either treated simultaneously with SAHA and Y-27632 for 24 h or, alternatively, the inhibitor was added for the last 24 of 48 h treatment with SAHA. Similarly to the effects in control cells, the ability of Y-27632 to reverse the increase in ACF induced by SAHA depended on the cell type: the simultaneous use of ROCK inhibitor always reduced the effect of SAHA in CML-T1 cells and sometimes in HL-60 cells. No effect of Y-27632 on SAHA-induced increase in cell adhesion was observed in Karpas-299 cells under the same experimental conditions while the inhibitor even potentiated the effect of SAHA in JURL-MK1 cells in some experiments. The effects of Y-27632 on the cell adhesion to FN are summarized in Table II.

We also tested the effects of other HDAC inhibitors, sodium butyrate and trichostatin A, on JURL-MK1 cell adhesion to FN. It follows from our in vitro measurements of HDAC activity in cell lysates that the efficiency of 0.5 mM sodium butyrate in HDAC inhibition is comparable to that of 0.5 μM SAHA (in both cases, the effect of the inhibitor reached the maximum value at this concentration, data not shown). We also previously reported that sodium butyrate induces erythroid differentiation without

TABLE II. Effects of ROCK Inhibition on the Cell Adhesion

Cell line	Effect on ACF in controls	Effect on SAHA-induced increase of ACF
JURL-MK1	No effect	Synergy/no effect
K562	No effect	No effect/synergy
Karpas-299	No effect	No effect
CML-T1	Decrease	Inhibition
HL-60	No effect/decrease	No effect/inhibition

To test the effects of Y-27632 on the adhesion of control cells, the inhibitor was added at 10 μM concentration for 16–24 h. To analyze the interference of Y-27632 with SAHA, the cells were treated with SAHA for 24 or 48 h and Y-27632 was added for the last 24 h of SAHA treatment. The adherent cell fraction (ACF) was then determined using the adhesion assay.

significant apoptosis in K562 cells at 0.6 mM concentration while it triggers apoptosis at 2 mM concentration [Grebeňová et al., 2006]. However, no increase in the cell adhesivity to FN could be detected after K562 or JURL-MK1 cell treatment with sodium butyrate at up to 2 mM concentration. Similarly, based on the in vitro inhibition constants, 100 nM trichostatin A should have similar effect on HDAC activity as 2 mM sodium butyrate. We found that 500 nM trichostatin-induced cell cycle arrest, cell death, and decrease of cell adhesion to FN in JURL-MK1 cells (data not shown). However, no increase in JURL-MK1 adhesion to FN was detected at lower concentrations of trichostatin A. Thus, it seems that the increase in cell adhesion to FN is specific for SAHA.

DISCUSSION

We performed the analysis of toxic effects induced by SAHA in different leukemic cell lines and in lymphocytes obtained from healthy donors. The sensitivity of the individual cell types to SAHA was variable: HL-60 cells undergo extensive and fast apoptosis which is strongly concentration-dependent (Fig. 1). Caspase activation (Fig. 2B) and apoptotic DNA fragmentation (Fig. 1) also occur to a large extent in JURL-MK1 and CML-T1 cells, as well as in donor lymphocytes. Karpas-299 cells appear to be relatively resistant to apoptosis as judged from limited caspase-3 activation and TUNEL-positive cell fraction but they undergo other form of cell death as indicated by the high fraction of Trypan blue-positive cells after 48 h treatment with SAHA (Fig. 3). On the other hand, K562 cells resist well to SAHA at up to 2 μM concentration. These findings support the view that the mechanism of SAHA action is complex and the resulting effect greatly depends on the individual cell context. It appears that the variability in the responses to SAHA is not related to the cell line origin (type of disease) as three CML-derived cell lines (JURL-MK1, CML-T1, and K562) behave quite differently.

Despite of this different sensitivity of the individual cell types to SAHA-induced cell death, SAHA had consistent effects on the cell adhesion to FN when it was added at subtoxic concentration (0.5 μM). The protocol we used to determine the ACF allows for reliable detection of changes as small as several percent and we show that 48 h treatment with 0.5 μM SAHA increases 1.5- to 2.5-fold the cell adhesion to FN in six different leukemia/lymphoma-derived cell lines but not in normal lymphocytes (Table I). For comparison, JURL-MK1 cell treatment with phorbol-myristoylacetate (PMA, 50 nM, 30 min), an activator of protein kinase C which is known to enhance the cellular adhesivity to ECM, induced (1.8 ± 0.7) fold increase in the cell adhesivity to FN (mean and standard deviation from eight experiments, data not shown) under our experimental conditions. A slight increase in the cell adhesivity resulting from 0.5 μM SAHA treatment was also observed in primary samples from CML patients. The effect was weaker than for the cell lines, probably because the peripheral blood of patients in early stage of CML contains a mixture of normal (prevalent) and transformed cells [Kuželová et al., 2006].

Increasing SAHA concentration to toxic doses usually led to the loss of elevatory effect on ACF (Fig. 5). It is known that the early stages of apoptosis include cell rounding and detachment from the ECM and surrounding cells [Shi and Wei, 2007; Taylor et al., 2008]. Although the mechanism of these processes is not fully elucidated, the positive effect of SAHA on the cell adhesivity can be counteracted by the changes related to apoptosis or other form of cell death which is induced by SAHA at higher concentration (Figs. 1 and 3).

SAHA-induced increase in the cell adhesivity to FN can be at least in part mediated by an increase in the expression level of integrin β1 on the cell surface which was observed in four out of five cell lines tested (Fig. 6). The only exception is represented by HL-60 cells and it could be due to the fact that in these cells SAHA triggers apoptosis already at 0.5 μM concentration. This can oppose some of the effects promoting the cell adhesion to FN. The surfacial density of integrin molecules is not the only parameter involved in the regulation of cellular adhesivity to FN: for example, the ability of integrins to cluster and to initiate the formation of functional focal adhesion complexes is of crucial importance. Nevertheless, our results suggest that SAHA can enhance the cell adhesion to FN through the upregulation of integrin β1 expression, which we observed both on the transcriptional and translational level (Fig. 8).

Paxillin is an adaptor protein which directly binds to integrins and serves as a scaffold for many other components of focal adhesion complexes (e.g., focal adhesion kinase, FAK, or vinculin). It can be phosphorylated at several sites, for example, by Src kinase, and enhanced paxillin phosphorylation on tyrosines 31 and 118 is observed upon the cell adhesion to ECM [Schaller and Schaefer, 2001]. We found that the treatment of leukemic cells with 0.5 μM SAHA elevates the expression level of paxillin (Fig. 7). The upregulation of paxillin was confirmed also at the transcriptional level (Fig. 8A) although the increase in paxillin mRNA is less marked in comparison with that of the protein level. Thus, SAHA treatment probably also results in higher stability of paxillin protein product. The increased availability of this essential constituent of focal adhesions after cell treatment with SAHA can contribute to a more efficient cell adhesion to FN. Paxillin was also shown to be cleaved by caspases during cell apoptosis [Chay et al., 2002]. This can result in focal adhesion disassembly and may explain the loss of SAHA effect on the cell adhesivity at higher concentrations of the drug. In keeping with the absence of SAHA effects on the adhesion of normal cells, no change in paxillin expression occurred upon SAHA addition to normal lymphocytes.

Firm adhesion of adherent cells to ECM involves the formation of actin stress fibers, which consists of 10–30 filaments of polymeric actin cross-linked by alpha-actinin, nonmuscle myosin, and tropomyosins [Pellegrin and Mellor, 2007]. These cytoskeletal structures are connected to ECM network through the focal adhesions and help to maintain mechanical resistance of the cell to detachment from ECM [Butler et al., 2006]. Integrin engagement leads to the activation of small GTPase RhoA which stimulates the formation of stress fibers and focal adhesions [Kabuyama et al., 2006; Villalonga and Ridley, 2006]. Among the main effectors of RhoA, the proteins ROCK1 and ROCK2 activate LIM kinase which in turn inactivates by phosphorylation the actin depolymerizing factor cofilin and thereby provides stabilization of actin structures [Bernard, 2007]. On the other hand, phosphorylation of myosin light chain also induced by ROCK proteins stimulates the

contractility of actin–myosin fibers. ROCK is required for the maturation of focal adhesions [Nagamatsu et al., 2008] and the inhibition of ROCK function using pharmacological inhibitors or expression of dominant-negative mutant results in disassembly of stress fibers and of focal adhesions in fibroblasts and epithelial cells. The function of RhoA/ROCK is less clear in hematopoietic cells which do not form robust actin fibers and the relation between the cytoskeletal arrangement and the cellular adhesivity to ECM is less obvious. Nevertheless, the adhesion of hematopoietic cells to FN is accompanied by changes in conformation and in lateral motility of β integrins and their clustering. As in the adherent cells, the intracellular parts of integrins become the base of complex protein structures which include small Rho GTPases and actin structure-forming proteins [Gao et al., 2005; Butler et al., 2006]. However, several reports indicated that RhoA and ROCK activity rather impedes the adhesion of hematopoietic cells to ECM [Aepfelbacher, 1995; Lai et al., 2003; Lee and Chang, 2008].

We thus explored the involvement of ROCK proteins in the increased adhesion of leukemic cells due to SAHA treatment using the inhibitor Y-27632. The effect of Y-27632 on the amount of polymeric actin (detected by phalloidin staining) in control cells confirmed its efficiency in our cell lines (data not shown). The effect of ROCK inhibition on the adhesion of control as well as of SAHA-treated cells to FN was strongly dependent on the cell type (Fig. 9 and Table II). While the inhibitor had no effect on the adhesivity of Karpas-299 cells, it decreased ACF in both control and SAHA-treated HL-60 and CML-T1 cells. On the other hand, the inhibition of ROCK in some experiments with JURL-MK1 and K562 cells potentiated the effect of SAHA on the cell adhesion to FN. In general, ROCK activity is thus not required for the increase of leukemic cell adhesivity to FN induced by SAHA and, in agreement with the above mentioned reports, the inhibition of ROCK can even enhance the cellular adhesivity to FN in some cell types. In HL-60 and CML-T1 cells, the ability of Y-27632 to reduce ACF in SAHA-treated cells does not obviously prove the involvement of RhoA/ROCK pathway in the processes induced by SAHA. The inhibitor reduces ACF also in nontreated CML-T1 and HL-60 cells and ROCK-related and SAHA-related processes may have independent contributions to the cellular adhesivity.

The stimulation of cell adhesivity to FN we describe in this work is not only specific for transformed cells (no increase in ACF was observed in normal lymphocytes) but seems also to be limited to SAHA as we detected no change in ACF after JURL-MK1 and K562 cell treatment with sodium butyrate and even with trichostatin A which belongs to the same structural class as SAHA. Interestingly, both SAHA and sodium butyrate were previously reported to upregulate the expression of proteins involved in the cell–cell adhesion [Bordin et al., 2004]. One of the reports dealing with SAHA effects on the gene expression mentions the integrin alpha 2 (CD49b) among the genes with increased expression due to SAHA treatment [Peart et al., 2005].

Our results are somewhat contradictory to that of Mahlknecht and Schönbein [2008] who found that SAHA downregulated the expression of VLA-4 (i.e., integrin subunit α4, CD49d) in cell lines and primary cells derived from patients with AML and decreased the adhesion of KG1a cells (an AML cell line) to mesenchymal stromal cells. The authors did not observed any change in the expression of integrin β1 (CD29) in AML cells treated with SAHA. It is possible that the response of AML cells to SAHA is different from that of other cell types. Indeed, the only cell line which did not display increased integrin β1 expression after SAHA treatment in our experiments was an AML line (HL-60). Also, an exceptional experimental result, that is, SAHA-induced decrease in the cell adhesivity, was obtained only with primary cells from two (out of three) AML patients. Nevertheless, we found no difference between AML-derived and other cell lines in the adhesion experiments with FN (Table II). The decrease of KG1a cell adhesion to stromal cells due to SAHA reported by Mahlknecht and Schönbein was significant at 2 μM SAHA concentration and the authors did not examine the effect of SAHA on KG1a cell viability. Thus, the adhesivity decrease could also be a secondary effect of apoptosis triggered by SAHA treatment.

CONCLUSIONS

In addition to previously reported effects on the cell proliferation, differentiation, and viability, SAHA also alters adhesion properties of hematopoietic cells. The effects of SAHA on the cell adhesion occur already at low SAHA concentrations in leukemic but not in normal cells and seems to be specific for this particular HDAC inhibitor. On the contrary to the other SAHA-induced processes, which are highly cell type-dependent, the increase in the cell adhesivity occurs consistently in different types of leukemic cells.

The ability of SAHA to increase the adhesivity of transformed hematopoietic cells to FN should be taken into account whenever SAHA is considered for clinical use. The in vitro doses used in our study correspond to the lowest concentrations used in patients for clinical studies when SAHA is used as a single agent [Mahlknecht and Schönbein, 2008]. Our results show that low-dose SAHA, possibly used in combination with an anticancer drug, could cause higher retention of malignant cells in the bone marrow. It is known that the bone marrow microenvironment offers protection from many chemotherapeutic agents for normal and malignant hematopoietic cells as well as for disseminating cancer cells from epithelial tumors [Meads et al., 2008; Riethdorf et al., 2008]. Higher fraction of transformed cells thus could escape the effects of the anticancer treatment which would aggravate the residual disease and increase the risk of the disease relapse.

ACKNOWLEDGMENTS

The authors wish to thank H. Pilcová for the expert technical assistance.

REFERENCES

Aepfelbacher M. 1995. ADP-ribosylation of Rho enhances adhesion of U937 cells to fibronectin via the alpha 5 beta 1 integrin receptor. FEBS Lett 363:78–80.

Bernard O. 2007. Lim kinases, regulators of actin dynamics. Int J Biochem Cell Biol 39:1071–1076.

Bordin M, D'Atri F, Guillemot L, Citi S. 2004. Histone deacetylase inhibitors up-regulate the expression of tight junction proteins. Mol Cancer Res 2:692–701.

Brodská B, Otevřelová P, Kalousek I. 2009. Variations in c-Myc and p21WAF1 expression protect normal peripheral blood lymphocytes against BimEL-mediated cell death. Cell Biochem Funct 27:167–175.

Butler B, Gao C, Mersich AT, Blystone SD. 2006. Purified integrin adhesion complexes exhibit actin-polymerization activity. Curr Biol 16:242–251.

Chay K-O, Park SS, Mushinski JF. 2002. Linkage of caspase-mediated degradation of paxillin to apoptosis in Ba/F3 murine Pro-B lymphocytes. J Biol Chem 277:14521–14529.

Crump M, Coiffier B, Jacobsen ED, Sun L, Ricker JL, Xie H, Frankel SR, Randolph SS, Cheson BD. 2008. Phase II trial of oral vorinostat (suberoylanilide hydroxamic acid) in relapsed diffuse large-B-cell lymphoma. Ann Oncol 19:964–969.

Desmond JC, Raynaud S, Tung E, Hofmann WK, Haferlach T, Koeffler HP. 2007. Discovery of epigenetically silenced genes in acute myeloid leukemias. Leukemia 21:1026–1034.

Dokmanovic M, Clarke C, Marks PA. 2007. Histone deacetylase inhibitors: Overview and perspectives. Mol Cancer Res 5:981–989.

Duvic M, Vu J. 2007. Vorinostat: A new oral histone deacetylase inhibitor approved for cutaneous T-cell lymphoma. Expert Opin Invest Drugs 16: 1111–1120.

Gao C, Schaefer E, Lakkis M, Blystone SD. 2005. Beta3 tyrosine phosphorylation and alphaVbeta3-mediated adhesion are required for Vav1 association and Rho activation in leukocytes. J Biol Chem 280:15422–15429.

Gaymes TJ, Padua RA, Pla M, Orr S, Omidvar N, Chomienne C, Mufti GJ, Rassool FV. 2006. Histone deacetylase inhibitors (HDI) cause DNA damage in leukemia cells: A mechanism for leukemia-specific HDI-dependent apoptosis? Mol Cancer Res 4:563–573.

Gillenwater AM, Zhong M, Lotan R. 2007. Histone deacetylase inhibitor suberoylanilide hydroxamic acid induces apoptosis through both mitochondrial and Fas (Cd95) signaling in head and neck squamous carcinoma cells. Mol Cancer Ther 6:2967–2975.

Glaser KB, Staver MJ, Waring JF, Stender J, Ulrich RG, Davidsen SK. 2003. Gene expression profiling of multiple histone deacetylase (HDAC) inhibitors: Defining a common gene set produced by HDAC inhibition in T24 and MDA carcinoma cell lines. Mol Cancer Ther 2:151–163.

Grebeňová D, Kuželová K, Pluskalová M, Pešlová G, Halada P, Hrkal Z. 2006. The proteomic study of sodium butyrate antiproliferative/cytodifferentiation effects on K562 cells. Blood Cells Mol Dis 37:210–217.

Gui CY, Ngo L, Xu WS, Richon VM, Marks PA. 2004. Histone deacetylase (HDAC) inhibitor activation of p21WAF1 involves changes in promoter-associated proteins, including HDAC1. Proc Natl Acad Sci USA 101:1241–1246.

Haberland M, Montgomery RL, Olson EN. 2009. The many roles of histone deacetylases in development and physiology: Implications for disease and therapy. Nat Rev Gen 10:32–42.

Kabuyama Y, Langer SJ, Polvinen K, Homma Y, Resing KA, Ahn NG. 2006. Functional proteomics identifies protein-tyrosine phosphatase 1B as a target of RhoA signaling. Mol Cell Proteomics 5 (8): 1359–1367.

Kumagai T, Akagi T, Desmond JC, Kawamata N, Gery S, Imai Y, Song JH, Gui D, Said J, Koeffler HP. 2009. Epigenetic regulation and molecular characterization of C/EBPalpha in pancreatic cancer cells. Int J Cancer 124:827–833.

Kuželová K, Grebeňová D, Pluskalová M, Marinov I, Klamová H, Hrkal Z. 2006. Imatinib mesylate affects tyrosine kinase activity in both leukemic and normal primary mononuclear blood cells. J Appl Biomed 4:95–104.

Kuželová K, Grebeňová D, Hrkal Z. 2007. Labeling of apoptotic JURL-MK1 cells by fluorescent caspase-3 inhibitor FAM-DEVD-fmk occurs mainly at site(s) different from caspase-3 active site. Cytometry Part A 71A:605–611.

Lai J-M, Hsieh C-L, Chang Z-F. 2003. Caspase activation during phorbol ester-induced apoptosis requires ROCK-dependent myosin-mediated contraction. J Cell Sci 116:3491–3501.

Lee HH, Chang ZF. 2008. Regulation of RhoA-dependent ROCKII activation by Shp2. J Cell Biol 181:999–1012.

Lindemann RK, Newbold A, Whitecross KF, Frew LA, Ellis L, Williams S, Wiegmans AP, Dear AE, Scott CL, Pellegrini M, Wei A, Richon VM, Marks PA, Lowe SW, Smyth MJ, Johnstone RW. 2007. Analysis of the apoptotic and therapeutic activities of histone deacetylase inhibitors by using a mouse model of B cell lymphoma. Proc Natl Acad Sci USA 104:8071–8076.

Mahlknecht U, Schönbein C. 2008. Histone deacetylase inhibitor treatment downregulates VLA-4 adhesion in hematopoietic stem cells and acute myeloid leukemia blast cells. Haematologica 93:443–446.

Marks PA, Breslow R. 2007. Dimethyl sulfoxide to vorinostat: Development of this histone deacetylase inhibitor as an anticancer drug. Nat Biotechnol 25:84–90.

Marks PA, Jiang X. 2005. Histone deacetylase inhibitors in programmed cell death and cancer therapy. Cell cycle 4:549–551.

Meads MB, Hazlehurst LA, Dalton WS. 2008. The bone marrow microenvironment as a tumor sanctuary and contributor to drug resistance. Clin Cancer Res 14:2519–2526.

Mitsiades CS, Mitsiades NS, Mcmullan CJ, Poulaki V, Shringarpure R, Hideshima T, Akiyama M, Chauhan D, Munshi N, Gu X, Bailey C, Joseph M, Libermann TA, Richon VM, Marks PA, Anderson KC. 2004. Transcriptional signature of histone deacetylase inhibition in multiple myeloma: Biological and clinical implications. Proc Natl Acad Sci USA 101:540–545.

Modesitt SC, Sill M, Hoffman JS, Bender DP. 2008. A phase II study of vorinostat in the treatment of persistent or recurrent epithelial ovarian or primary peritoneal carcinoma: A Gynecologic Oncology Group study. Gynecol Oncol 109:182–186.

Monneret C. 2005. Histone deacetylase inhibitors. Eur J Med Chem 40:1–13.

Nagamatsu Y, Rikitake Y, Takahashi M, Deki Y, Ikeda W, Hirata K, Takai Y. 2008. Roles of Necl-5/poliovirus receptor and Rho-associated kinase (ROCK) in the regulation of transformation of integrin alpha(V)beta(3)-based focal complexes into focal adhesions. J Biol Chem 283:14532–14541.

O'Connor OA, Heaney ML, Schwartz L, Richardson S, Willim R, MacGregor-Cortelli B, Curly T, Moskowitz C, Portlock C, Horwitz S, Zelenetz AD, Frankel S, Richon V, Marks PA, Kelly WK. 2006. Clinical experience with intravenous and oral formulations of the novel histone deacetylase inhibitor suberoylanilide hydroxamic acid in patients with advanced hematologic malignancies. J Clin Oncol 24:166–173.

Peart MJ, Smyth GK, Van Laar RK, Bowtell DD, Richon VM, Marks PA, Holloway AJ, Johnstone RW. 2005. Identification and functional significance of genes regulated by structurally different histone deacetylase inhibitors. Proc Natl Acad Sci USA 102:3697–3702.

Pellegrin S, Mellor H. 2007. Actin stress fibers. J Cell Sci 120:3491–3499.

Richardson P, Mitsiades C, Colson K, Reilly E, McBride L, Chiao J, Sun L, Ricker J, Rizvi S, Oerth C, Atkins B, Fearen I, Anderson K, Siegel D. 2008. Phase I trial of vorinostat (suberoylanilide hydroxamic acid, SAHA) in patients with advanced multiple myeloma. Leuk Lymphoma 49:502–507.

Riethdorf S, Wikman H, Pantel K. 2008. Biological relevance of disseminated tumor cells in cancer patients. Int J Cancer 123:1991–2006.

Rosato RR, Grant S. 2004. Histone deacetylase inhibitors in clinical development. Expert Opin Invest Drugs 13:21–38.

Ruefli AA, Bernhard D, Tainton KM, Kofler R, Smyth MJ, Johnstone RW. 2002. Suberoylanilide hydroxamic acid (SAHA) overcomes multidrug resistance and induces cell death in P-glycoprotein-expressing cells. Int J Cancer 99:292–298.

Schaller MD, Schaefer EM. 2001. Multiple stimuli induce tyrosine phosphorylation of the Crk-binding sites of paxillin. Biochem J 360:57–66.

Shao Y, Gao Z, Marks PA, Jiang X. 2004. Apoptotic and autophagic cell death induced by histone deacetylase inhibitors. Proc Natl Acad Sci USA 101: 18030–18035.

Shi J, Wei L. 2007. Rho kinase in the regulation of cell death and survival. Arch Immunol Ther Exp 55:61–75.

Tavares TS, Nanus D, Yang XJ, Gudas LJ. 2008. Gene microarray analysis of human renal cell carcinoma: The effects of HDAC inhibition and retinoid treatment. Cancer Biol Ther 7:1607–1618.

Taylor RC, Cullen SP, Martin SJ. 2008. Apoptosis: Controlled demolition at the cellular level. Nat Rev Mol Cell Biol 9:231–241.

Tong A, Zhang H, Li Z, Gou L, Wang Z, Wei H, Tang M, Liang S, Chen L, Huang C, Wei Y. 2008. Proteomic analysis of liver cancer cells treated with suberoylanilide hydroxamic acid. Cancer Chemother Pharmacol 61:791–802.

Villalonga P, Ridley AJ. 2006. Rho GTPases and cell cycle control. Growth Factors 24:159–164.

Xu WS, Parmigiani RB, Marks PA. 2007. Histone deacetylase inhibitors: Molecular mechanism of action. Oncogene 26:5541–5552.

Yu C, Dasmahapatra G, Dent P, Grant S. 2005. Synergistic interactions between MEK1/2 and histone deacetylase inhibitors in BCR/ABL+ human leukemia cells. Leukemia 19:1579–1589.